Accepted Manuscript

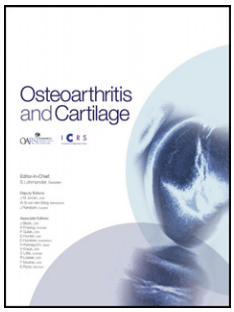

Title: Increased chondrocyte sclerostin may protect against cartilage degradation in osteoarthritis

Authors: B.Y Chan, E.S Fuller, A Russell, S.S Smith, M.M Smith, M.T Jackson, M.A Cake, R.A Read, J.F Bateman, P.N Sambrook, C.B Little

PII: S1063-4584(11)00131-2

DOI: 10.1016/j.joca.2011.04.014

Reference: YJOCA 2453

To appear in: *Osteoarthritis and Cartilage*

Received Date: 29 November 2010

Accepted Date: 20 April 2011

Please cite this article as: Chan BY, Fuller ES, Russell A, Smith SS, Smith MM, Jackson MT, Cake MA, Read RA, Bateman JF, Sambrook PN, Little CB. Increased chondrocyte sclerostin may protect against cartilage degradation in osteoarthritis, Osteoarthritis and Cartilage (2011), doi: 10.1016/j.joca.2011.04.014

Increased chondrocyte sclerostin may protect against cartilage degradation in osteoarthritis

[1]Chan BY, [1]Fuller ES, [1]Russell A, [1]Smith SS, [1]Smith MM, [1]Jackson MT, [3]Cake MA, [3]Read RA, [2]Bateman JF, [1]Sambrook PN, [1]Little CB

[1]*Raymond Purves Bone and Joint Research Labs, Kolling Institute of Medical Research, Institute of Bone and Joint Research, University of Sydney, Royal North Shore Hospital, St. Leonards, NSW 2065.*

[2]*Murdoch Childrens Research Institute, Parkville, Victoria 3052, Australia.*

[3]*School of Veterinary and Biomedical Sciences, Murdoch University, Perth, WA 6150, Australia*

Running Title: Sclerostin in osteoarthritic cartilage

Corresponding Author

A/Prof Christopher Little

Address: Raymond Purves Bone and Joint Research Lab

L10 Kolling Building – B6

Royal North Shore Hospital

St Leonards NSW 2065

Australia

Email: Christopher.little@sydney.edu.au

Total word count: 3,992

Abstract

***Objectives*:** To investigate the regulation of sclerostin (SOST) in osteoarthritis (OA) and its potential effects on articular cartilage degradation.

Methods: SOST and other Wnt-β-catenin components were immuno-localised in osteochondral sections of surgically-induced OA in knees of sheep and mice, and human OA samples obtained at arthroplasty. Regulation of *SOST* mRNA and protein expression by ovine chondrocytes in response to interleukin-1α (IL-1α) or tumor necrosis factor-α (TNFα) was examined in explant cultures. The effect of 25 or 250ng/ml recombinant SOST alone or in combination with IL-1α, on ovine articular cartilage explant aggrecan degradation, and chondrocyte gene expression of Wnt-β-catenin pathway proteins, metalloproteinases and their inhibitors, and cartilage matrix proteins was quantified. .

Results: Contrary to being an osteocyte-specific protein, *SOST* was expressed by articular chondrocytes, and mRNA levels were upregulated in vitro by IL-1α but not TNFα. Chondrocyte SOST staining was significantly increased only in the focal area of cartilage damage in surgically-induced OA in sheep and mice, as well as end-stage human OA. In contrast, osteocyte SOST was focally decreased in the subchondral bone in sheep OA in association with bone sclerosis. SOST was biologically active in chondrocytes, inhibiting Wnt-β-catenin signalling and catabolic metalloproteinase (MMP and ADAMTS) expression, but also decreasing mRNA levels of aggrecan, collagen II and TIMPs. Despite this mixed effect, SOST dose-dependently inhibited IL-1α-stimulated cartilage aggrecanolysis in vitro.

***Conclusions*:** These results implicate SOST in regulating the OA disease processes, but suggest opposing effects by promoting disease-associated subchondral bone sclerosis while inhibiting degradation of cartilage.

Key words: sclerostin, β-catenin, MMPs, ADAMTS, cartilage, osteoarthritis

Introduction

The aetiology of knee osteoarthritis (OA) is multifactorial, and although ageing is strongly associated, other factors contribute. In particular altered biomechanics and joint instability commonly leads to "post-traumatic OA" within 10-15 years after joint injury in humans [1, 2]. The central feature of OA is considered to be the progressive destruction of articular cartilage, however change occurs in all joint tissues. Subchondral bone thickening and marginal osteophytosis are classic features of OA, and together with synovitis correlate with pain [3]. Focal loss of articular cartilage in OA may be linked to changes in the subjacent bone, through altered load transmission and/or direct signalling between the adjacent tissues [4].

The Wnt-β-catenin signalling pathway has well-recognised roles in embryology and development, and is emerging as critical regulator of bone and cartilage homeostasis in the adult [5-8]. Canonical Wnt signalling is initiated by binding to frizzled receptors and co-receptors, (low-density lipoprotein receptor (LRP) 5/6), which leads to β-catenin stabilization, nuclear translocation, and activation of target genes such as Wnt-induced signalling protein-1 (*WISP1).* Wnt signalling is modulated by soluble antagonists including dickkopf-1 (DKK1), secreted frizzled-related proteins (sFRPs), and sclerostin (SOST) [6]. There is a large body of evidence demonstrating the central role for Wnt signalling in regulating adult bone turnover, with increased β-catenin activity inducing bone production, and inhibition of soluble antagonists an emerging therapeutic approach for osteoporotic and inflammatory bone loss [7, 9]. In adult cartilage in contrast, increased Wnt-β-catenin stimulates tissue breakdown rather than formation [10]. WISP1 is increased in OA, and when over-expressed induces cartilage degradation by upregulating matrix metalloproteinases (MMPs) and aggrecanases [11]. The pro-degradative effects of Wnt-β-catenin are also driven through promotion of chondrocyte hypertrophy and the associated upregulation of MMPs [6, 8]. Induction of constitutive β-catenin activity in adult mouse chondrocytes causes progressive cartilage degeneration and

increased subchondral bone density [12]. Circulating DKK1 levels negatively correlate with biomarkers of cartilage breakdown in OA patients [13] and sFRP3 knockout mice have augmented cartilage proteoglycan loss in a collagenase-induced instability model of arthritis [14].

Collectively this data suggests that elevated β-catenin activity is a common mechanism in the excess bone formation and overlying cartilage loss in OA. However, the complexity of Wnt-β-catenin regulation and effects on joint tissues is demonstrated by the fact that constitutive *inhibition* of chondrocyte β-catenin activity also leads to OA in mice [15]. Increased circulating DKK1 (i.e reduced Wnt-β-catenin) is associated with worse cartilage degradation in rheumatoid patients [13]. DKK1 promotes chondrocyte apoptosis *in vitro* [16], which may explain the reduction in severity in rat OA models with systemic DKK1 inhibition [17]. The conflicting data with DKK1 blockade being chondroprotective while sFRP3 ablation augments chondrolysis, may suggest distinct roles for different Wnt inhibitors in different tissues and/or disease states (e.g. degree of inflammation). The effect on OA of blocking SOST, the other important soluble inhibitor of Wnt signalling, has not been reported.

Sclerostin, is a member of the DAN/Cerberus protein family and acts to inhibit BMP secretion from cells in which it is co-expressed, and as a potent inhibitor of canonical Wnt signaling by binding to LRP5/6 [18, 19]. It is the failure to inhibit Wnt-β-catenin signaling that accounts for the characteristic high bone density phenotypes in patients with homozygous defects in *SOST* [20], and in *Sost* knock out mice [21]. Sclerostin expression is down regulated by mechanical loading of bone [22] but can be induced by pro-inflammatory cytokines [23, 24], indicating that SOST can regulate both mechanical and inflammatory bone remodeling. There is little information on changes in SOST in arthritis, with a reduction in the number of SOST-positive osteocytes noted in association with increased cortical bone density in the femoral neck of patients with hip OA [25], and in zygapophyseal joints with

OA and ankylosing spondylitis [26]. Recently it has been demonstrated that SOST is also expressed by chondrocytes in mineralized cartilage [27], and in human end-stage OA [28]. To date there has been no analysis of changes in SOST in subchondral bone in OA and how this relates to the overlying cartilage damage. Furthermore, the regulation of SOST expression by chondrocytes, the effects of SOST on chondrocytes and whether SOST plays any role in cartilage degradation has not previously been studied. The aim of this study is to investigate these questions to better define the role of SOST in OA.

Materials and Methods

Animal models and human specimens

Four-year-old castrated male Merino sheep underwent unilateral medial meniscectomy (MEN) (n=6) or a sham procedure (arthrotomy alone; n=6) three months prior to euthanasia with institutional ethics approval (AEC832R/00) [29]. Coronal 5mm-thick osteochondral specimens spanning the width of the medial tibial plateau encompassing the region of maximal cartilage damage and adjacent unaffected tissues, were fixed for 24 hours (10% neutral-buffered formalin), decalcified (10% formic acid/5% formalin) and paraffin embedded [30].

Ten-week-old male C57BL/6 mice underwent destabilization of the medial meniscus (DMM) and sham surgery in right and left knees, respectively [31, 32], with institutional ethics approval (protocols 0051-005A and 0506-019A). Four mice were euthanised 1, 2 and 6 weeks after surgery. Sagittal sections every 40µ across the width of the medial femoro-tibial joint were evaluated [33] enabling intervening sections with maximal OA change to be used for immunohistochemistry.

Human specimens were obtained with informed consent and approval of the Northern Sydney Health Human Research Ethics Committee, from patients undergoing total knee replacement for OA. Sections (4µm) from formalin-fixed, decalcified, paraffin-embedded coronal osteochondral specimens spanning the width of the medial tibial plateaus and encompassing the focal area of maximal cartilage erosion from 9 patients were immunostained (see below). Pooled residual articular cartilage from the tibial plateau was harvested from an additional 6 patients and RNA extracted [34].

Histopathology and immunohistochemistry

Sections from ovine joints were stained with toluidine blue and fast green, and the cartilage degradation scored (BC and CBL) using a previously described grading system [30]. The cartilage damage was scored in two separate regions (Fig 1A): area 1 = unprotected, and area 2 = normally protected by the meniscus, the latter experiencing increased loading and degeneration following meniscectomy while area 1 remains unaffected (Fig 1A) [35]. The density of subchondral bone in area 1 and 2 was quantified from digital images of haematoxylin and eosin stained serial sections. A region of interest 1.1 mm wide x 3.4 mm deep spanned the maximal depth of the subchondral bone plate (chondro-osseous junction to the beginning of trabecular bone). The % of this area containing eosin-stained bone was quantified (Image-Pro Plus 5.1; Media Cybernetics, Bethesda, USA), as a measure of "subchondral bone density".

Sections for immunostaining were dewaxed and rehydrated, and incubated in Protein-Block-Serum-Free (X909; DakoCytomation) for ten minutes at room temperature. Sections were immunolocalised overnight at 4°C with primary antibody or non-immune serum or IgG as negative controls, using conditions optimised from preliminary studies: rabbit anti-sclerostin (Abcam, UK) 1.25µg/ml; goat anti-sclerostin (R&D systems, USA) and rabbit anti-WISP1 (Santa Cruz, USA) 1µg/ml. Secondary antibody incubation and colour development were performed as described [35]. Coded digital images were evaluated independently by two observers (BC and CBL) and the number of positively stained cells in each region were quantified. The specificity of the anti-sclerostin antibody was demonstrated by pre-absorption with 10x concentration of recombinant human SOST for 2hr at room temperature before routine immunohistochemistry.

Ex-vivo cartilage explants culture

Full-depth articular cartilage explants (5-10mm^2, ~40mg) from the trochlear groove of 6-12 month-old ovine knee joints were cultured in serum free media for 24 and 48 hours ± 10ng/mL IL-1α or 100ng/mL TNFα (PeproTech, Rocky Hill, NJ) [36]. The effect of SOST was examined by addition of 25 or 250ng/mL of rhSOST (R&D Systems, Minneapolis, USA) for 48 hours ± 10ng/mL IL-1α. At harvest the explants were blotted dry, weighed, and snap-frozen in liquid nitrogen for RNA extraction. Release of glycosaminoglycan (GAG) into the media was measured using dimethylmethylene blue and normalised to the explant wet weight [36].

RNA extraction, reverse transcription and real-time quantitative PCR

Approximately 100mg of frozen ovine or human cartilage were fragmented in a Mikro-Dismembrator (Braun Biotech International, Melsungen, Germany). Total RNA was extracted with TRIzol and isolated using the RNeasy kit (Qiagen, Australia) including an on-column DNase I (Qiagen) digestion, quantified with a Nanodrop 1000 spectrophotometer (Thermo Scientific, Waltham, USA), and samples with a 260/280 ratio >2.0 used for reverse transcription (RT). Changes in mRNA expression were quantified using real time qRT-PCR as described [37] using specific primer sets (Table 1). The "housekeeping genes" examined (GAPDH, HRPT, β-actin and ubiquitin) were all regulated by one or more of the experimental conditions (data not shown), and therefore samples were normalised using equal amounts of total RNA as recommended [38, 39], and effects of treatment expressed as fold change from control.

Statistical analysis

Data is reported as mean with 95% confidence intervals (lower, upper). Ordinal data (histological scoring) is presented graphically in box plots showing median, upper and lower

quartile (box), 10-90th percentile (whiskers) and maximum and minimum values. Changes in the number of positively stained cells, and the fold change in gene expression or GAG release are presented graphically as mean with 95% confidence intervals. Because some data (e.g. gene expression) was not normally distributed, all treatment effects were assessed using non-parametric analysis (Mann-Whitney *U* test) with $P < 0.05$ considered significant.

Results

Sclerostin is increased in cartilage but decreased in subchondral bone in OA

Medial meniscectomy induced focal OA-like change in the sheep, including loss of cartilage proteoglycan, cartilage surface fibrillation and partial thickness erosion, and marginal osteophytosis (Fig 1A). Significant cartilage changes were restricted to the region previously protected by the meniscus that is subjected to high focal loading in meniscectomised joints (Area 2 – score 3.2 (2.4,3.9) vs 10.4 (8.6,12.2); $p<0.001$), with no change in Area 1 (Fig 1B). In association with the overlying cartilage damage there was increased subchondral bone in Area 2 in meniscectomised joints (Fig 1C, 80.1% (74.1,86.1) vs 92.8% (86.4,99.2); $p=0.018$).

Sclerostin was immunolocalised to osteocytes and their canaliculi in the subchondral plate (Fig 1D) and deeper trabecular bone (not shown) in sham-operated joints. This staining was specific as demonstrated by lack of signal when IgG was substituted for the primary antibody (not shown) or pre-absorption with rhSOST prior to immunostaining (Fig 1E). There was no difference in the number of SOST-positive osteocytes between Area 1 and 2 in sham-operated joints, although both were greater than trabecular bone (Fig 1F; Area 1 = 71.0% (66.8,77.2), Area 2 = 67.9% (65.1,70.7) vs trabecular bone 29.5% (15.9,43), $p=0.002$ for both). There was little SOST staining of chondrocytes in the non-calcified cartilage in sham-operated joints (Fig 1D), while some hypertrophic chondrocytes in the calcified cartilage were positive (not shown). In meniscectomised joints osteocyte SOST staining intensity decreased in Area 2 subchondral bone with little change in Area 1 (Fig 1D) or trabecular bone (not shown). The percentage of SOST-positive osteocytes in subchondral bone decreased in meniscectomised joints (Fig 1F) in Area 1 (57.9% (49.5,66.3), $p=0.019$ versus sham) and Area 2 (46.2% (32.7,59.8), $p=0.012$ versus sham). In contrast, there was a marked increase in SOST staining intensity (Fig 1D), and the number of positive chondrocytes in the

non-calcified cartilage only in Area 2 in meniscectomised joints (Fig 1F; 15.0% (7.2,22.9) vs 42.3% (23.1,61.4); p=0.001).

We confirmed the positive chondrocyte SOST immunostaining observed in sheep, in DMM-induced OA in mice and in late stage human OA (Fig. 2). In sham-operated mouse joints, there was no SOST staining in non-calcified articular cartilage chondrocytes, although almost all chondrocytes in the calcified cartilage were immunopositive (Fig 2A). At 2 weeks post-DMM, scattered chondrocytes in the non-calcified cartilage became SOST positive, and there was an increase in staining intensity in the calcified cartilage (Fig 2A). In 3/9 human OA tibial plateaux, chondrocytes in the superficial cartilage zones, often in clusters, stained strongly for SOST (Fig 2B). The antibody specificity was confirmed by osteocytes in subchondral and trabecular bone having typical SOST staining, and the lack of staining when IgG was substituted for the primary antibody (Fig 2B).

Chondrocytes express Sost mRNA and it is regulated by IL-1

We investigated whether the SOST staining in chondrocytes was associated with local synthesis by the chondrocytes rather than diffusion of exogenous protein into the cartilage. We detected *SOST* mRNA in chondrocytes in ovine cartilage, and from 2/6 human patients tested (Fig 2C). We examined whether the increase chondrocytes SOST in OA might be due to upregulated expression by inflammatory cytokines. In preliminary studies equivalent maximal GAG release from cartilage occurred with 10ng/ml IL-1α and 100ng/ml TNFαdatanotshowñAtthese maximally effective doses, IL-1α induced a 9-fold (6.6,10.7) up-regulation of *SOST* compared with control at 24 hours (Fig 3A; p<0.001), and this remained elevated at 48 hours (1.8-fold (1.3,2.2); p=0.093). This IL-1-induced increase in *SOST* mRNA was accompanied by increased chondrocyte SOST immuno-localization (Fig 3B). In

contrast, TNFα did not alter chondrocyte *SOST* expression in ovine cartilage explants at either 24 or 48 hours (Fig 3A).

Wnt-β-catenin signalling is altered in meniscectomy-induced OA in sheep

In light of SOST being an antagonist of Wnt-β-catenin signalling in bone, we examined whether WISP1, a down-stream indicator of β-catenin activity, was co-ordinately decreased in the sheep OA model. In sham-operated joints WISP1 was immunolocalised to osteocytes in the subchondral bone plate (Fig 4A) and trabecular bone (not shown). There was no difference in the number of WISP1-positive osteocytes between bone regions in sham-operated joints and no change following meniscectomy (Fig 4B). WISP1 was immunolocalised to the chondrocytes in the superficial layer in sham-operated joints (Fig 4A), and some hypertrophic chondrocytes in the calcified cartilage (not shown). Following meniscectomy there was no change in intensity or distribution of chondrocyte WISP1 staining in Area 1, however chondrocytes through the depth of the non-calcified cartilage showed strong staining in Area 2 (Fig 4A). The percentage of WISP1-positive chondrocytes increased only in Area 2 of meniscectomized joints (22.0% (15.5,28.4) versus 56.6% (38.0,75.2); p=0.006; Fig 4B).

SOST regulates gene expression in normal cartilage

The co-localised increase in chondrocyte SOST and WISP1 staining in OA cartilage (Area 2) were not consistent with the purported role of SOST as an inhibitor of Wnt-β-catenin signalling. We therefore investigated the effect of SOST on chondrocyte expression of *WISP1* as a marker of β-catenin activity, as well as a number of other Wnt-signalling genes in normal ovine cartilage explants. Treatment with 25 or 250ng/mL rhSOST for 24 hours did not regulate *WISP1* expression (not shown). However, significant suppression of *WISP1* as

well as *CTNNB1, LRP5 and LRP6* was noted after 48 hours incubation with both doses of SOST (Fig 5A). Concordant with this inhibition of Wnt signalling at 48 hours, SOST decreased *COL2*, *ACAN* and *TIMP1* mRNA expression by a similar level at both doses (Fig 5B). *MMP1* and *ADAMTS4* mRNA levels were not significantly altered by SOST suggesting that the effects were not due to generalised cell toxicity. *MMP13* expression was decreased only at the lowest dose while *ADAMTS5* and *TIMP3* were dose-dependently decreased.

SOST inhibits IL-1-induced cartilage degradation

The results in normal cartilage suggest that indeed SOST is a negative regulator of Wnt-β-catenin signalling and activity in chondrocytes. However SOST had effects on chondrocyte gene expression that would be considered "anti-anabolic" (decreased *ACAN* and *COL2*), "pro-catabolic" (decreased *TIMP1* and *TIMP3*) as well as "anti-catabolic" (decreased *MMP13* and *ADAMTS5*). In order to investigate the effect of SOST in an environment where cartilage catabolism is augmented, we co-cultured explants for 48 hours with SOST in the presence of 10ng/ml IL-1α. IL-1α induced the expected changes in chondrocyte gene expression, decreasing *ACAN* and *COL2* while increasing *MMP1, MMP13, ADAMTS4* and *ADAMTS5* (Fig 6A). These IL-1-induced changes were accompanied by increased GAG release and a concordant loss of toluidine blue staining of the cartilage (Fig 6B). Importantly, SOST dose-dependently decreased IL-1α-induced GAG release into the media, with over 50% reduction at 250ng/ml (Fig 6B, $p<0.001$), albeit that it still remained elevated compared with control cultures. SOST still decreased Wnt-β-catenin signalling in the presence of IL-1α as indicated by the reduction in *WISP1* expression with the 250 ng/ml dose (0.45-fold (0.25,0.65), $p=0.009$). SOST also inhibited expression of other Wnt-β-catenin signalling molecules in the presence of IL-1, with *CTNNB1* reduced at both 25ng/ml (0.35-fold (0.1,0.6); $p=0.003$) and 250ng/ml (0.4-fold (0.2,0.6); $p=0.005$), and the other genes at 250ng/ml only

(LRP5 0.4-fold (0.2,0.6), p=0.029; LRP6 0.25-fold (0.01,0.49), p=0.12). This inhibition of Wnt-β-catenin signalling and GAG release by SOST was associated with significant down-regulation of IL-1α-induced chondrocyte expression of *MMP1*, *MMP13*, *ADAMTS4* and *ADAMTS5*, while the IL-1-induced inhibition of *ACAN* and *COL2* remained unchanged (Fig 6C).

Discussion

Canonical Wnt signalling and increased β-catenin activity has been implicated in the process of cartilage degradation in OA [11, 40]. The current data from the sheep meniscectomy model of OA supports these previous studies, showing elevated chondrocyte WISP-1 staining. Our detailed regional analysis enabled us to demonstrate that this increase in WISP-1 was restricted to the chondrocytes in the focal area of cartilage degradation, and was unaltered in the remaining cartilage or the subjacent bone. Previous studies have suggested conflicting roles for DKK1 and sFRP3 in regulating cartilage and bone changes in animal models of OA [14, 17]. SOST is also a potent Wnt antagonist and a key regulator of bone metabolism, but no previous publications have investigated whether it plays a role in global OA joint pathology. We have for the first time demonstrated an increase in SOST in chondrocytes restricted to the focal area of cartilage degradation in post-traumatic OA. In addition, we found a differential regulation in cartilage and bone, with a decrease in osteocyte SOST staining associated with increased subchondral plate thickening. Furthermore, we show that chondrocytes themselves express *SOST* which can be regulated by IL-1α but not TNFα. SOST could act as an inhibitor of Wnt-β-catenin signalling in chondrocytes *in vitro*, and in the presence of IL-1α significantly regulate expression of cartilage matrix proteins, MMPs, ADAMTS and TIMPs, with a net result of reducing IL-1α-induced aggrecanolysis. Taken together, this data suggests that changes in SOST may play a role in the pathological progression of OA, promoting subchondral bone sclerosis but potentially inhibiting cartilage proteolysis.

Given that SOST is a potent antagonist of the Wnt-β-catenin pathway, it is difficult to reconcile the coincident increase in SOST and WISP-1 in OA cartilage. One possible explanation is that β-catenin is being activated in chondrocytes by prostaglandin-E2,

independent of Wnt-signalling as described in other cell types [41]. Canonical regulation of β-catenin by Wnts is complex, with levels of different Wnts, receptors, inhibitors and intracellular ligands all contributing [42]. A decrease in one of these components may be offset by the increase in another, with a net abrogation of the expected action. Nevertheless, the increase in SOST in OA chondrocytes should be acting to decrease canonical signalling, and most data suggests that elevated chondrocyte β-catenin has a pro-catabolic effect on cartilage, stimulating MMP and ADAMTS synthesis via increased WISP-1 [11, 16], and promoting chondrocyte hypertrophy which is associated with OA cartilage pathology [6, 8]. As such, elevated chondrocyte SOST is likely to be at least partially chondroprotective, and in its absence an even greater increase in chondrocyte β-catenin activity, WISP1 and associated cartilage degradation would ensue. Our *in vitro* data support this hypothesis, with down regulation of β-catenin signalling, MMP and ADAMTS expression by SOST. Consistent with a beneficial effect of Wnt antagonism, elevated circulating levels of DKK1 are negatively associated with serum markers of cartilage degradation in human OA [13]. However, it would appear that some "appropriate" level of chondrocyte β-catenin activity is needed to maintain normal cartilage, as excessive inhibition [12] and *in vitro* treatment with DKK1 [16], can induce chondrocyte apoptosis and cartilage breakdown.

The effect of SOST on Wnt signalling in OA cartilage/chondrocytes will be dependent on its binding to Lrp5/6. DKK1 can displace SOST from Lrp5/6 [43], and a concurrent increase in both of these proteins in OA cartilage could potentiate effects of SOST outside the Lrp5/6-β-catenin pathway. SOST binds to Lrp4, and hypomorphic mutations in Lrp4 result in skeletal abnormalities in mice including polysyndactyly, possibly through interfering with BMP signalling [43]. SOST also functions as a BMP antagonist by inhibiting secretion from cells in which it is co-expressed [18], and BMPs have potent effects on chondrogenesis,

chondrocyte maturation and anabolism [44], as well as increasing DKK1 expression [45]. Over expression of human *SOST* in mice leads not only to decreased bone density through inhibition of Wnt-β-catenin signalling, but also syndactyly consistent with inhibition of BMPs [46]. SOST can rapidly activate ERK1/2 signalling in osteoblasts by an undefined pathway [24]. These non-Wnt-dependent pathways may contribute to the effect of elevated SOST in OA chondrocytes, possibly promoting rather than inhibiting cartilage degradation.

Control of *SOST* expression by different regulatory elements in the proximal promoter is dependent on cell type [46]. Our *in vitro* data demonstrates that, at doses that induce cartilage degradation, IL-1α but not TNFα increased *SOST* expression. The lack of effect of TNFα on *SOST* mRNA levels in chondrocytes is interesting in light of the significant upregulation of *SOST* by TNFα in osteoblasts [24], consistent with cell-specific regulation. Regulation of chondrocyte type II collagen and MMP expression by IL-1 have been reported to be independent of Wnt-β-catenin signalling [11, 47]. Nevertheless both IL-1 and TNF can regulate expression and activity of the Wnt-β-catenin pathway [16, 24]. Our data demonstrating a distinct difference between IL-1α and TNFα in *SOST* regulation while the two cytokines have similar effects on *ACAN*, *COL2*, *MMP* and *ADAMTS* expression (data not shown), is consistent with cytokine-driven cartilage catabolism being independent of Wnt-β-catenin. Chondrocyte-derived IL-1 has been implicated in OA cartilage degradation [48], which could potentially account for the increase in SOST in OA cartilage. However, the very focal nature of the cartilage changes and altered SOST expression in our sheep OA model, suggests a more localized regulatory mechanism such as mechanical loading. In bone, *SOST* expression is strongly regulated by mechanical loading [22, 49], and the decrease in SOST protein in the subchondral plate following meniscectomy is consistent with these previous studies. Despite the overlying cartilage also experiencing increased focal compressive

loading in the meniscectomy model, an increase rather than decrease in chondrocyte SOST was seen. This may suggest different mechano-regulation of *SOST* in osteocytes versus chondrocytes. The reason that only ~30% of OA human cartilage samples expressed SOST mRNA and protein is unclear but could be associated with differences in the degree of synovial inflammation between patients. It may also be associated with disease chronicity and activity in end-stage human OA, with the normal SOST staining of osteocytes in human samples perhaps indicative of little active remodelling at the time of joint replacement. Nevertheless, the fact that articular chondrocytes expressed SOST in OA in all three species suggests it is a common pathophysiological mechanism, and future studies should examine the temporal changes in SOST over the course of OA initiation and progression.

In conclusion, we have demonstrated that contrary to being an osteocyte-specific product, *SOST* is expressed by articular chondrocytes and regulated by IL-1α. Importantly, chondrocyte SOST is focally increased in cartilage in OA while being decreased in the subjacent subchondral bone. While the role of SOST in regulating bone metabolism has been well established, we show for the first time that SOST is biologically active in chondrocytes, not only inhibiting Wnt-β-catenin signalling and catabolic MMP and ADAMTS expression, but also decreasing mRNA levels of key matrix components and enzyme inhibitors. Despite this mixed effect, SOST dose-dependently inhibited IL-1α-stimulated cartilage aggrecanolysis *in vitro*. These results implicate SOST in regulating the OA disease processes in both bone and cartilage, but suggest opposing effects by promoting disease-associated subchondral bone sclerosis while inhibiting degradation of cartilage. Increasing Wnt-β-catenin activity using antibodies to SOST (and DKK1) has potential in treating osteoporotic and inflammatory bone loss [50, 51]. While it is unlikely such therapeutic agents will enter cartilage to regulate chondrocyte SOST, given the multiple mechanisms of action of SOST in

joint tissues, it will be important to determine what effect its inhibition may have on progression of both bone and cartilage changes in OA *in vivo*.

Acknowledgments

This study was funded by NHMRC project grant 607399 and Dr Chan's salary was paid in part by the Alec Brenan Fellowship through the University of Sydney Medical Foundation.

Author contributions

All authors were involved in drafting the article or revising it critically for important intellectual content, and all authors approved the final version to be published.

Conflict of interest

There are no financial interests, direct or indirect, that might affect the content of this manuscript.

References

1. Roos H, Adalberth T, Dahlberg L, Lohmander LS. Osteoarthritis of the knee after injury to the anterior cruciate ligament or meniscus: the influence of time and age. Osteoarthritis Cartilage 1995;3:261-7.
2. Jacobsen K. Osteoarthrosis following insufficiency of the cruciate ligaments in man. A clinical study. Acta Orthop Scand 1977;48:520-6.
3. Felson DT. Developments in the clinical understanding of osteoarthritis. Arthritis Res Ther 2009;11:203.
4. Karsdal MA, Leeming DJ, Dam EB, Henriksen K, Alexandersen P, Pastoureau P, et al. Should subchondral bone turnover be targeted when treating osteoarthritis? Osteoarthritis Cartilage 2008;16:638-46.
5. Beyer C, Schett G. Pharmacotherapy: concepts of pathogenesis and emerging treatments. Novel targets in bone and cartilage. Best Pract Res Clin Rheumatol 2010;24:489-96.
6. Blom AB, van Lent PL, van der Kraan PM, van den Berg WB. To seek shelter from the WNT in osteoarthritis? WNT-signaling as a target for osteoarthritis therapy. Curr Drug Targets 2010;11:620-9.
7. Hoeppner LH, Secreto FJ, Westendorf JJ. Wnt signaling as a therapeutic target for bone diseases. Expert Opin Ther Targets 2009;13:485-96.
8. Kawaguchi H. Regulation of osteoarthritis development by Wnt-beta-catenin signaling through the endochondral ossification process. J Bone Miner Res 2009;24:8-11.
9. Diarra D, Stolina M, Polzer K, Zwerina J, Ominsky MS, Dwyer D, et al. Dickkopf-1 is a master regulator of joint remodeling. Nat Med 2007;13:156-63.
10. Yuasa T, Otani T, Koike T, Iwamoto M, Enomoto-Iwamoto M. Wnt/beta-catenin signaling stimulates matrix catabolic genes and activity in articular chondrocytes: its possible role in joint degeneration. Lab Invest 2008;88:264-74.
11. Blom AB, Brockbank SM, van Lent PL, van Beuningen HM, Geurts J, Takahashi N, et al. Involvement of the Wnt signaling pathway in experimental and human osteoarthritis: prominent role of Wnt-induced signaling protein 1. Arthritis Rheum 2009;60:501-12.
12. Zhu M, Tang D, Wu Q, Hao S, Chen M, Xie C, et al. Activation of beta-Catenin Signaling in Articular Chondrocytes Leads to Osteoarthritis-Like Phenotype in Adult beta-Catenin Conditional Activation Mice. J Bone Miner Res 2009;23:10.
13. Voorzanger-Rousselot N, Ben-Tabassi NC, Garnero P. Opposite relationships between circulating Dkk-1 and cartilage breakdown in patients with rheumatoid arthritis and knee osteoarthritis. Ann Rheum Dis 2009;68:1513-4.
14. Lories RJ, Peeters J, Bakker A, Tylzanowski P, Derese I, Schrooten J, et al. Articular cartilage and biomechanical properties of the long bones in Frzb-knockout mice. Arthritis Rheum 2007;56:4095-103.
15. Zhu M, Chen M, Zuscik M, Wu Q, Wang YJ, Rosier RN, et al. Inhibition of beta-catenin signaling in articular chondrocytes results in articular cartilage destruction. Arthritis Rheum 2008;58:2053-64.
16. Weng LH, Wang CJ, Ko JY, Sun YC, Su YS, Wang FS. Inflammation induction of Dickkopf-1 mediates chondrocyte apoptosis in osteoarthritic joint. Osteoarthritis Cartilage 2009;17:919-29.
17. Weng LH, Wang CJ, Ko JY, Sun YC, Wang FS. Control of Dickkopf-1 ameliorates chondrocyte apoptosis, cartilage destruction and subchondral bone deterioration in osteoarthritic knee. Arthritis Rheum 2010.

18. Krause C, Korchynskyi O, de Rooij KE, Weidauer SE, de Gorter DJ, van Bezooijen RL, et al. Distinct modes of inhibition by Sclerostin on bone morphogenetic protein and Wnt signaling pathways. J Biol Chem 2010.
19. Semenov M, Tamai K, He X. SOST is a ligand for LRP5/LRP6 and a Wnt signaling inhibitor. J Biol Chem 2005;280:26770-5.
20. van Bezooijen RL, Roelen BA, Visser A, van der Wee-Pals L, de Wilt E, Karperien M, et al. Sclerostin is an osteocyte-expressed negative regulator of bone formation, but not a classical BMP antagonist. J Exp Med 2004;199:805-14.
21. Li X, Ominsky MS, Niu QT, Sun N, Daugherty B, D'Agostin D, et al. Targeted deletion of the sclerostin gene in mice results in increased bone formation and bone strength. J Bone Miner Res 2008;23:860-9.
22. Robling AG, Niziolek PJ, Baldridge LA, Condon KW, Allen MR, Alam I, et al. Mechanical stimulation of bone in vivo reduces osteocyte expression of Sost/sclerostin. J Biol Chem 2008;283:5866-75.
23. Heiland GR, Zwerina K, Baum W, Kireva T, Distler JH, Grisanti M, et al. Neutralisation of Dkk-1 protects from systemic bone loss during inflammation and reduces sclerostin expression. Ann Rheum Dis 2010;69:2152-9.
24. Vincent C, Findlay DM, Welldon KJ, Wijenayaka AR, Zheng TS, Haynes DR, et al. The Proinflammatory Cytokines TNF-related Weak Inducer of Apoptosis (TWEAK) and TNFalpha Induce the Mitogen Activated Protein Kinase (MAPK)-Dependent Expression of Sclerostin in Human Osteoblasts. J Bone Miner Res 2009;17:17.
25. Power J, Poole KE, van Bezooijen R, Doube M, Caballero-Alias AM, Lowik C, et al. Sclerostin and the regulation of bone formation: Effects in hip osteoarthritis and femoral neck fracture. J Bone Miner Res 2010;25:1867-76.
26. Appel H, Ruiz-Heiland G, Listing J, Zwerina J, Herrmann M, Mueller R, et al. Altered skeletal expression of sclerostin and its link to radiographic progression in ankylosing spondylitis. Arthritis Rheum 2009;60:3257-62.
27. van Bezooijen RL, Bronckers AL, Gortzak RA, Hogendoorn PC, van der Wee-Pals L, Balemans W, et al. Sclerostin in mineralized matrices and van Buchem disease. J Dent Res 2009;88:569-74.
28. Karlsson C, Dehne T, Lindahl A, Brittberg M, Pruss A, Sittinger M, et al. Genome-wide expression profiling reveals new candidate genes associated with osteoarthritis. Osteoarthritis Cartilage 2010;18:581-92.
29. Armstrong S, Read R, Ghosh P. The effects of intraarticular hyaluronan on cartilage and subchondral bone changes in an ovine model of early osteoarthritis. J Rheumatol 1994;21:680-8.
30. Little CB, Smith MM, Cake MA, Read RA, Murphy MJ, Barry FP. The OARSI histopathology initiative - recommendations for histological assessments of osteoarthritis in sheep and goats. Osteoarthritis Cartilage 2010;18 Suppl 3:S80-92.
31. Little C, Meeker C, Golub S, Lawlor K, Farmer P, Smith S, et al. Blocking aggrecanase cleavage in the aggrecan interglobular domain abrogates cartilage erosion and promoters cartilage repair. J Clin Invest 2007;117:1627.
32. Glasson SS, Blanchet TJ, Morris EA. The surgical destabilization of the medial meniscus (DMM) model of osteoarthritis in the 129/SvEv mouse. Osteoarthritis Cartilage 2007;15:1061-9.
33. Little CB, Barai A, Burkhardt D, Smith SM, Fosang AJ, Werb Z, et al. Matrix metalloproteinase 13-deficient mice are resistant to osteoarthritic cartilage erosion but not chondrocyte hypertrophy or osteophyte development. Arthritis Rheum 2009;60:3723-33.

34. Young AA, Appleyard RC, Smith MM, Melrose J, Little CB. Dynamic biomechanics correlate with histopathology in human tibial cartilage: a preliminary study. Clin Orthop Relat Res 2007;462:212-20.
35. Little C, Smith S, Ghosh P, Bellenger C. Histomorphological and immunohistochemical evaluation of joint changes in a model of osteoarthritis induced by lateral meniscectomy in sheep. J Rheumatol 1997;24:2199-209.
36. Jackson MT, Smith MM, Smith SM, Jackson CJ, Xue M, Little CB. Activation of cartilage matrix metalloproteinases by activated protein C. Arthritis Rheum 2009;60:780-91.
37. Smith MM, Sakurai G, Smith SM, Young AA, Melrose J, Stewart CM, et al. Modulation of aggrecan and ADAMTS expression in ovine tendinopathy induced by altered strain. Arthritis Rheum 2008;58:1055-66.
38. Bustin SA. Absolute quantification of mRNA using real-time reverse transcription polymerase chain reaction assays. J Mol Endocrinol 2000;25:169-93.
39. Bustin SA. Quantification of mRNA using real-time reverse transcription PCR (RT-PCR): trends and problems. J Mol Endocrinol 2002;29:23-39.
40. Dell'accio F, De Bari C, Eltawil NM, Vanhummelen P, Pitzalis C. Identification of the molecular response of articular cartilage to injury, by microarray screening: Wnt-16 expression and signaling after injury and in osteoarthritis. Arthritis Rheum 2008;58:1410-21.
41. Liu XH, Kirschenbaum A, Weinstein BM, Zaidi M, Yao S, Levine AC. Prostaglandin E2 modulates components of the Wnt signaling system in bone and prostate cancer cells. Biochem Biophys Res Commun 2010;394:715-20.
42. Corr M. Wnt-beta-catenin signaling in the pathogenesis of osteoarthritis. Nat Clin Pract Rheumatol 2008;4:550-6.
43. Choi HY, Dieckmann M, Herz J, Niemeier A. Lrp4, a novel receptor for Dickkopf 1 and sclerostin, is expressed by osteoblasts and regulates bone growth and turnover in vivo. PLoS ONE 2009;4:e7930.
44. Aigner T, Soeder S, Haag J. IL-1beta and BMPs--interactive players of cartilage matrix degradation and regeneration. Eur Cell Mater 2006;12:49-56; discussion 56.
45. Grotewold L, Ruther U. The Wnt antagonist Dickkopf-1 is regulated by Bmp signaling and c-Jun and modulates programmed cell death. EMBO J 2002;21:966-75.
46. Loots GG, Kneissel M, Keller H, Baptist M, Chang J, Collette NM, et al. Genomic deletion of a long-range bone enhancer misregulates sclerostin in Van Buchem disease. Genome Res 2005;15:928-35.
47. Ryu JH, Chun JS. Opposing roles of WNT-5A and WNT-11 in interleukin-1beta regulation of type II collagen expression in articular chondrocytes. J Biol Chem 2006;281:22039-47.
48. Kobayashi M, Squires GR, Mousa A, Tanzer M, Zukor DJ, Antoniou J, et al. Role of interleukin-1 and tumor necrosis factor alpha in matrix degradation of human osteoarthritic cartilage. Arthritis Rheum 2005;52:128-35.
49. Lin C, Jiang X, Dai Z, Guo X, Weng T, Wang J, et al. Sclerostin Mediates Bone Response to Mechanical Unloading via Antagonizing Wnt/beta-Catenin Signaling. J Bone Miner Res 2009;6:6.
50. Li X, Ominsky MS, Warmington KS, Morony S, Gong J, Cao J, et al. Sclerostin antibody treatment increases bone formation, bone mass, and bone strength in a rat model of postmenopausal osteoporosis. J Bone Miner Res 2009;24:578-88.
51. Deal C. Potential new drug targets for osteoporosis. Nat Clin Pract Rheumatol 2009;5:20-7.

Figure Legends

Figure 1. (**A**) Representative toluidine blue fast green stained section of a sheep tibial plateau 3 months post meniscectomy showing the separate areas of cartilage with adjacent subchondral bone (area 1 & 2), and deeper trabecular bone (TB) examined in subsequent analyses. The approximate dimensions of the marginal osteophyte is outlined in red and indicated with an arrow. High magnification images showing typical cartilage pathological changes in Area 1 and 2 in sham versus meniscectomised joints are shown on the right. (**B**) Modified Mankin score of tibial cartilage and **(C)** percentage of the subchondral region that was bone, in area 1 and 2 of sham-operated and meniscectomised (MEN) joints (line = median, box = upper and lower quartiles, whiskers = 10-90th percentile, circles = maximum and minimum values; n = 6 in both groups). (**D**) Representative sections showing immunlocalization of sclerostin (brown stain) in area 2 articular cartilage and adjacent subchondral bone in sham-operated and meniscectomised (MEN) joints. (**E**) Loss of SOST immunostaining in cartilage from MEN and bone from sham-operated joints by pre-absorption of the antibody with recombinant SOST. (**F**) The percentage of cells in different areas of sham-operated and MEN joints that were immunopositive for sclerostin (mean ± 95% confidence intervals; n = 6 in both groups). Significant difference between sham and MEN joints in different regions are indicated by a bar with the p-value given above.

Figure 2. (A) Sclerostin immunostaining in mouse knee joints 2 weeks after sham surgery or destabilization of the medial meniscus (DMM). Positive sclerostin staining (brown) was seen in osteocytes (black arrow) and hypertrophic chondrocytes in calcified cartilage (yellow arrow) in sham and DMM joints, Chondrocytes in the non-calcified articular cartilage (red arrow) were only immunopositive in DMM joints. **(B)** Representative sections of human

osteoarthritic cartilage and trabecular bone showing clusters of chondrocytes in the fibrillated surface and osteocytes that were immunopositive for sclerostin (brown stain), with no positive staining observed in serial sections with equal concentration of (1.25mg/mL) of IgG as a negative control. (C) Ethidium bromide stained gels showing expression of *SOST* mRNA by PCR, in 2 of 6 human OA articular cartilage samples.

Figure 3. (A) Quantitative PCR analysis of *SOST* gene expression in ovine articular cartilage explants cultured for 24 and 48 hours in serum free media alone (Control) or in the presence of IL-1α (10ng/ml) or TNFα (100ng/ml). Data is expressed as fold change in expression compared with untreated control cultures at each time point (mean ± 95% confidence intervals; n = 6 per treatment per time point). Significant differences compared to control culture at the same time is indicated by the p-value above the given culture condition. **(B)** Immuno-localization of SOST in ovine articular cartilage explants cultured for 24 hours in serum free media alone (Control) or in the presence of IL-1α (10ng/ml). Chondrocytes with positive SOST staining (brown stain) are indicated with red arrows.

Figure 4. Representative sections of ovine tibial plateau area 2 from sham and meniscectomised (MEN) joints, showing (**A**) WISP-1 immunolocalization (brown stain). (**B**) The percentage of cells in different areas of sham-operated and MEN joints that were immunopositive for WISP-1 (mean ± 95% confidence intervals; n = 6 in both groups). Significant differences between sham and MEN joints in different regions are indicated by a bar with the p-value given above.

Figure 5. Quantitative PCR analysis in ovine articular cartilage explants cultured for 48 hours in serum free media ± 25 or 250ng/ml recombinant human sclerostin. Expression of **(A)** Wnt-β-catenin pathway genes, and **(B)** matrix protein, metalloproteinase and tissue inhibitor genes. Data is expressed as fold change in expression compared with untreated control cultures (mean ± 95% confidence intervals; n = 22 replicates from 3 individual experiments). Significant differences compared to control culture is indicated by the p-value.

Figure 6. Effect of recombinant sclerostin (25 or 250ng/ml) on ovine articular cartilage cultured for 48 hours in the presence of 10ng/ml IL-1α. **(A)** Quantitative PCR analysis demonstrating the effect of IL-1 alone on the expression of matrix proteins, metalloproteinase and tissue inhibitors. Data is expressed as fold change in expression compared with untreated control cultures (mean ± 95% confidence intervals; n = 17 replicates from 3 individual experiments). (**B**) Representative images of toluidine blue stained sections of cartilage explants cultured for 48 hours ± 10ng/ml IL-1 ± 25 or 250ng/ml sclerostin. Sulphated glygosaminoglycan (GAG) release from the same cartilage cultures expressed as fold change in expression compared with untreated control cultures (mean ± 95% confidence intervals; n = 18 replicates from 3 individual experiments). (**C**) Quantitative PCR analysis demonstrating the effect of 25 or 250 ng/ml sclerostin in the presence 10ng/ml IL-1, on the expression of matrix proteins, metalloproteinase and tissue inhibitors. Data is expressed as fold change in expression compared with IL-1 alone (mean ± 95% confidence intervals; n = 17 replicates from 3 individual experiments). Significant differences compared to control culture are indicated by the p-value above or below the specific treatment. Differences between particular treatments connected by a bar are indicated by the p-value.

Species	Gene	Accession #	Tm (°C)	Product Size (bp)	Forward	Reverse
Ovine	*Agn*	U76615	58	105	TCACCATCCCCTGCTACTTCATC	TCTCCTTGGAAATGCGGCTC
	Adamts4	NM181667	60	149	AACTCGAAGCAATGCACTGGT	TGCCCGAAGCCATTGTCTA
	Adamts5	AF192771	55	97	GCATTGACGCATCCAAACCC	CGTGGTAGGTCCAGCAAACAGTTAC
	Col2	X02420	55	154	TGACCTGACGCCCATTCATC	TTTCCTGTCTCTGCCTTGACCC
	Mmp-1	AF267156	55	122	CATTCTACTGACATTGGGGCTCTG	TGAGTGGGATTTTGGGAAGGTC
	Mmp-13	AY091604.1	58	113	TGACAGGCAGACTTGATGATAAC	CATTTTGGACCACTTGAGAGTTC
	Timp1	S67450	57	265	GGT TCAGTGCCTTGAGAGATGC	GGGATAGATGAGCAGGGAAACAC
	Timp3	NM174473	57	286	CTTCCTTTGCCCTTCTCTACCC	TCTGGTCAACCCAAGCATCG
	Ctnnb1	NM_001076141.1	58	105	AATGGCTTGGAATGAGACTGCT	CCAGAGTGAAAAGAACGATAGC
	Dkk1	XM_580572.4	58	116	TCTTCGCTCATCAGACTGTGCTG	AGCCTTTTCTCCTGTGCTTGGTG
	Wisp1	XM_585338.3	58	290	ATCAAGGTGGGGAAGAAGTG	GAGAAGTCAGGGTAGGAGTC
	Lrp5	AB257751.1	58	335	ACTTCATCTACTGGACCGACTG	CACATCGTTGTTGTTGGTGTC
	Lrp6	AB257752.1	58	220	CGTCAAGTAGTTCATCAAGCACC	GCATAGTCACTGTCACACACATCTG
Ovine / Human	*Sost*	NM008078.1/XM588605.3	58	71	ACCACCCCTTTGAGACCAAAG	GGTCACGTAGCGGGTGAAGT

Figure 1

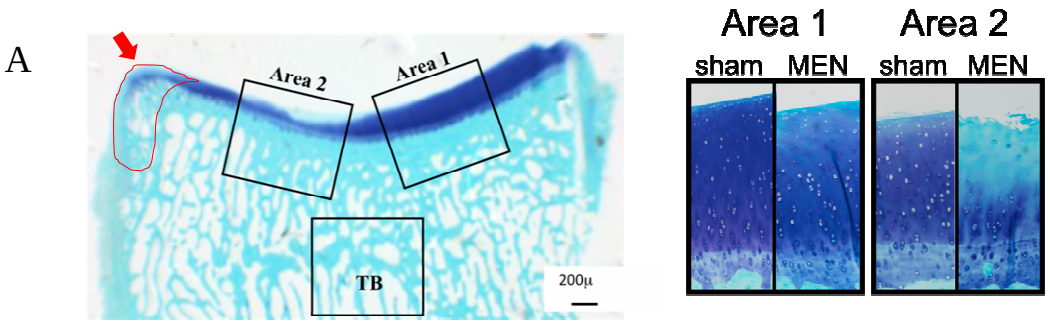
A
Area 2
Area 1
TB
200µ
Area 1
Area 2
sham
MEN
sham
MEN

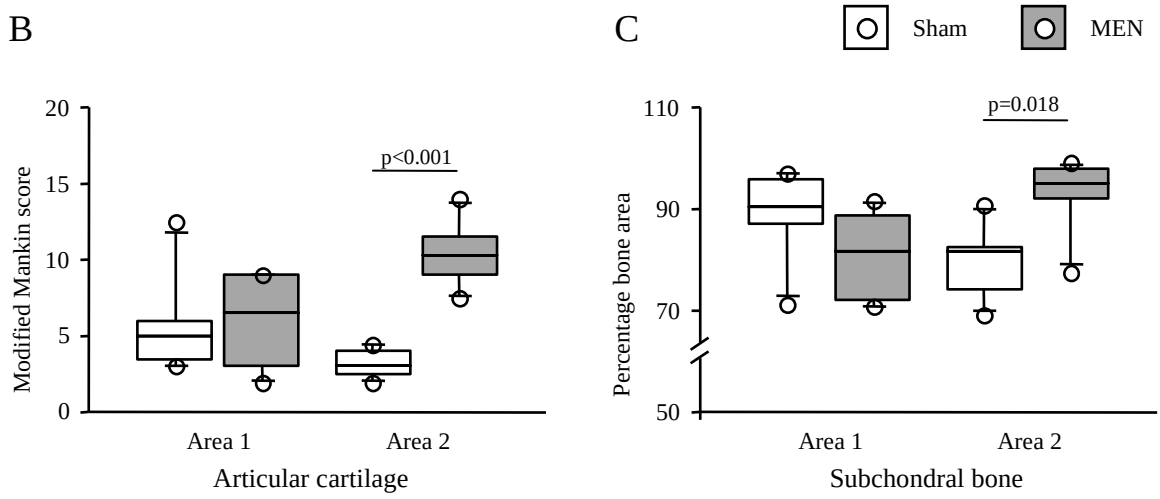
B
Modified Mankin score
20
15
10
5
0
p<0.001
Area 1
Area 2
Articular cartilage
C
Sham
MEN
Percentage bone area
110
90
70
50
p=0.018
Area 1
Area 2
Subchondral bone

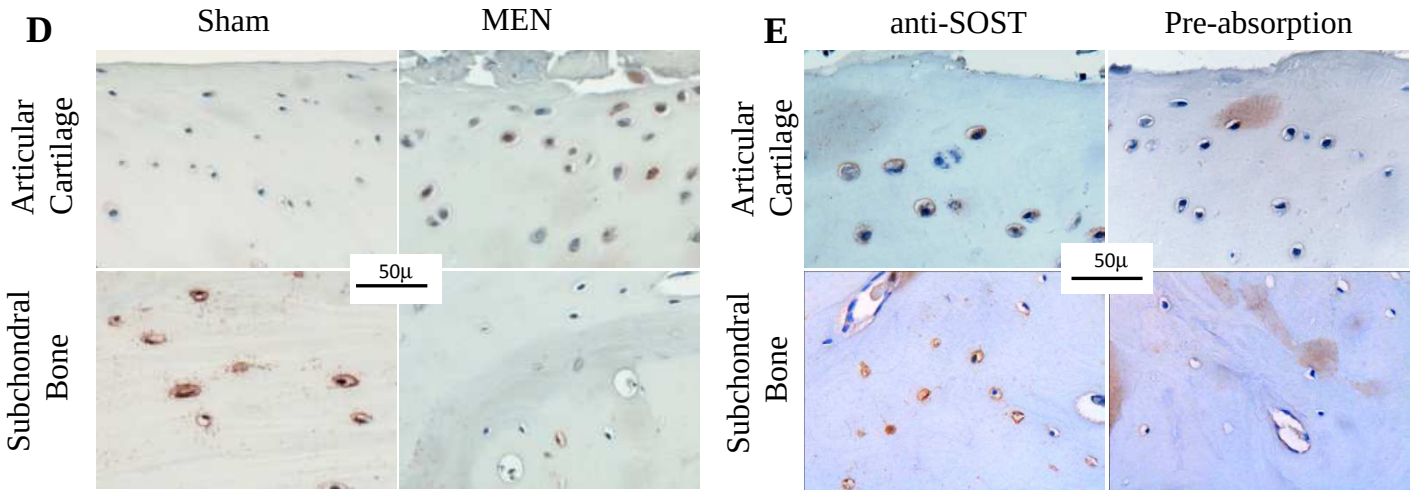
D
Sham
MEN
Articular Cartilage
Subchondral Bone
50µ
E
anti-SOST
Pre-absorption
Articular Cartilage
Subchondral Bone
50µ

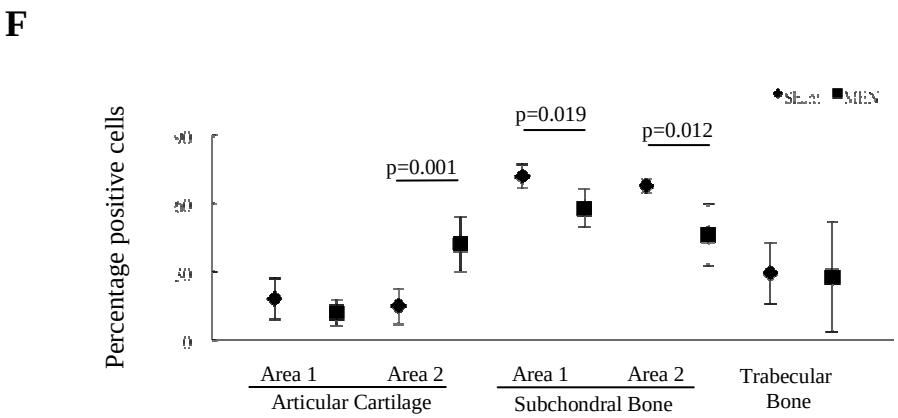
F
Percentage positive cells
p=0.001
p=0.019
p=0.012
Area 1
Area 2
Articular Cartilage
Area 1
Area 2
Subchondral Bone
Trabecular Bone

Figure 2

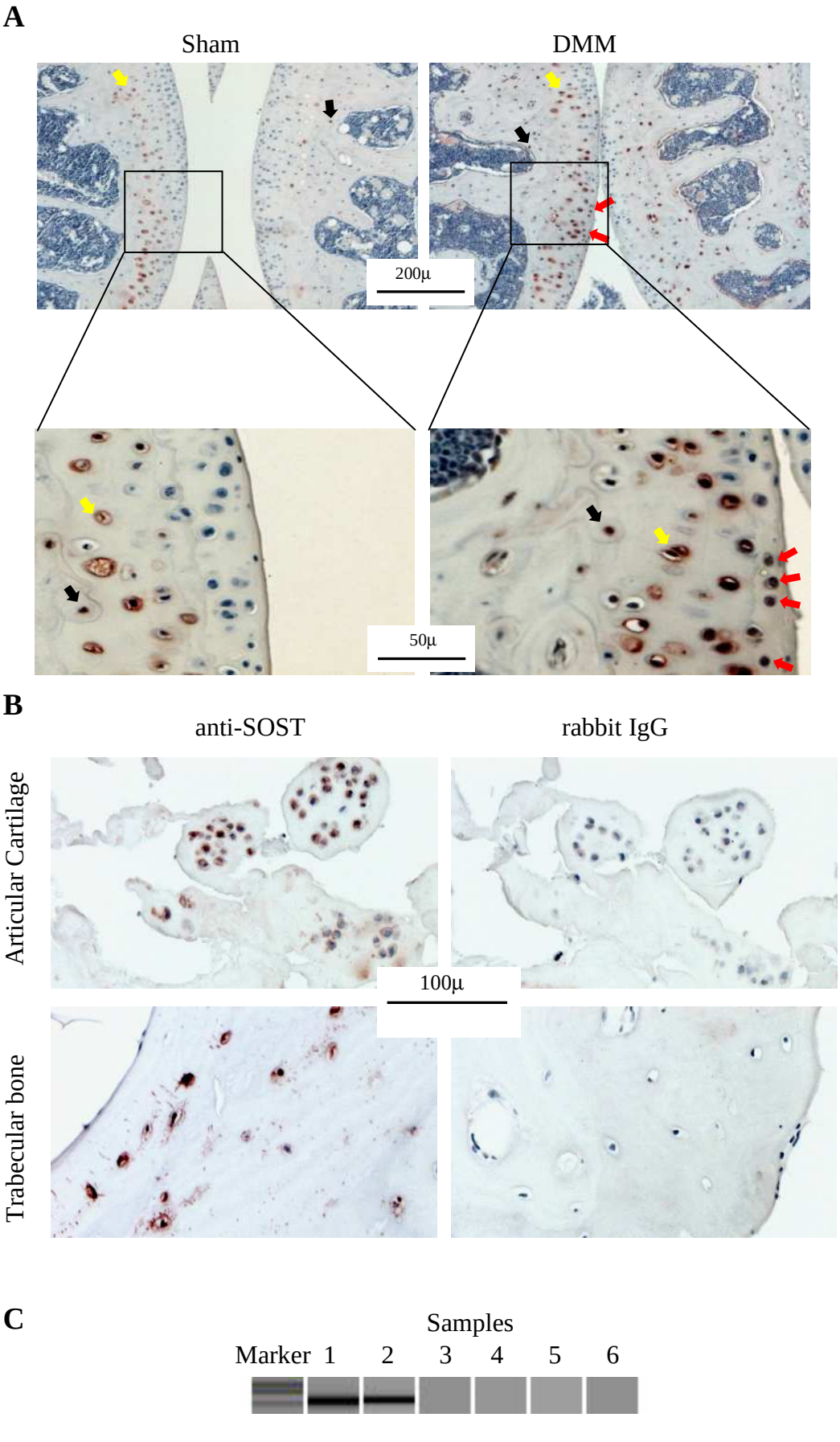
A
Sham
DMM
200μ
50μ
B
anti-SOST
rabbit IgG
Articular Cartilage
100μ
Trabecular bone
C
Samples
Marker 1 2 3 4 5 6

Figure 3

A

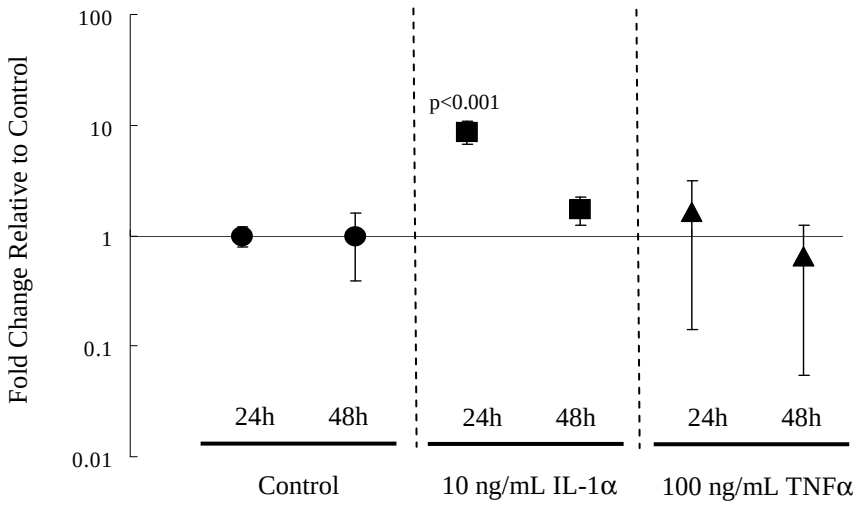
Fold Change Relative to Control
100
10
1
0.1
0.01
p<0.001
24h
48h
24h
48h
24h
48h
Control
10 ng/mL IL-1α
100 ng/mL TNFα

B

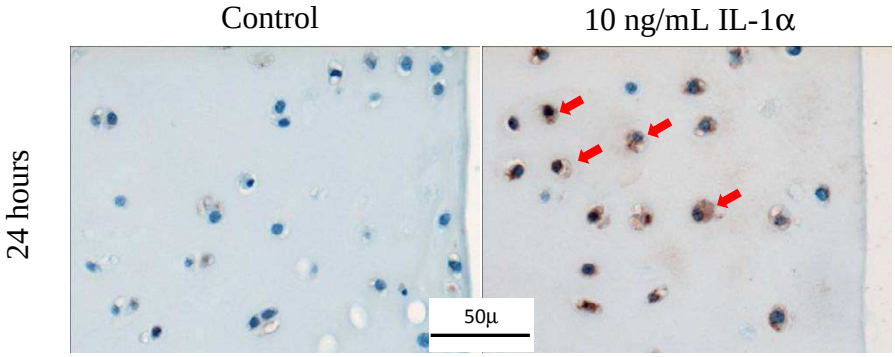
Control
10 ng/mL IL-1α
24 hours
50µ

Figure 4

A

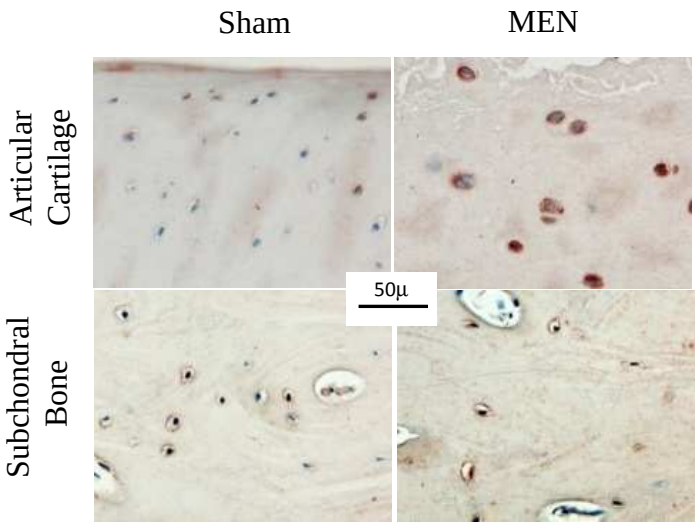
Sham
MEN
Articular Cartilage
Subchondral Bone
50µ

B

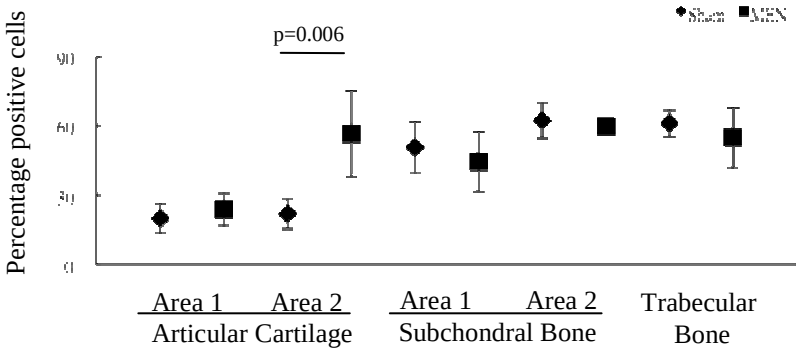
Percentage positive cells
p=0.006
Area 1
Area 2
Articular Cartilage
Area 1
Area 2
Subchondral Bone
Trabecular Bone

Figure 5

A

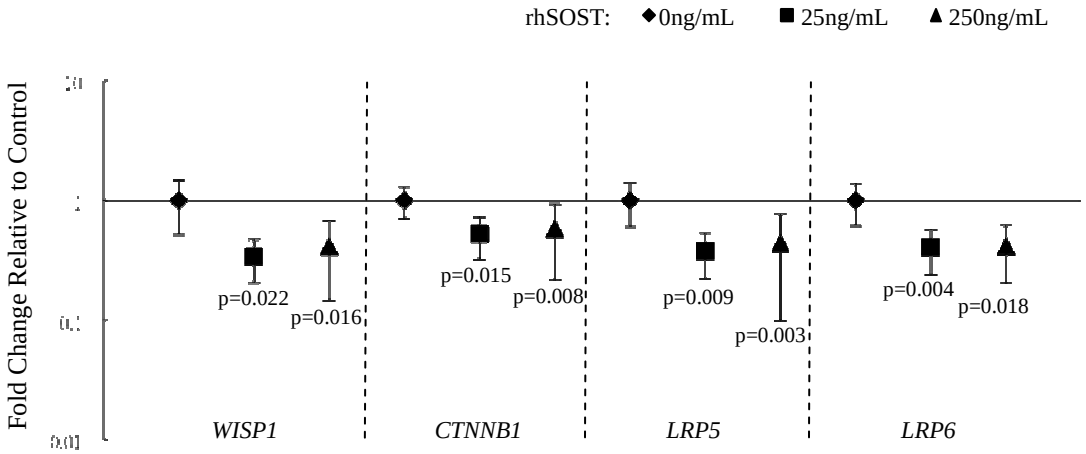
rhSOST: 0ng/mL 25ng/mL 250ng/mL
Fold Change Relative to Control
p=0.022
p=0.016
p=0.015
p=0.008
p=0.009
p=0.003
p=0.004
p=0.018
WISP1
CTNNB1
LRP5
LRP6

B

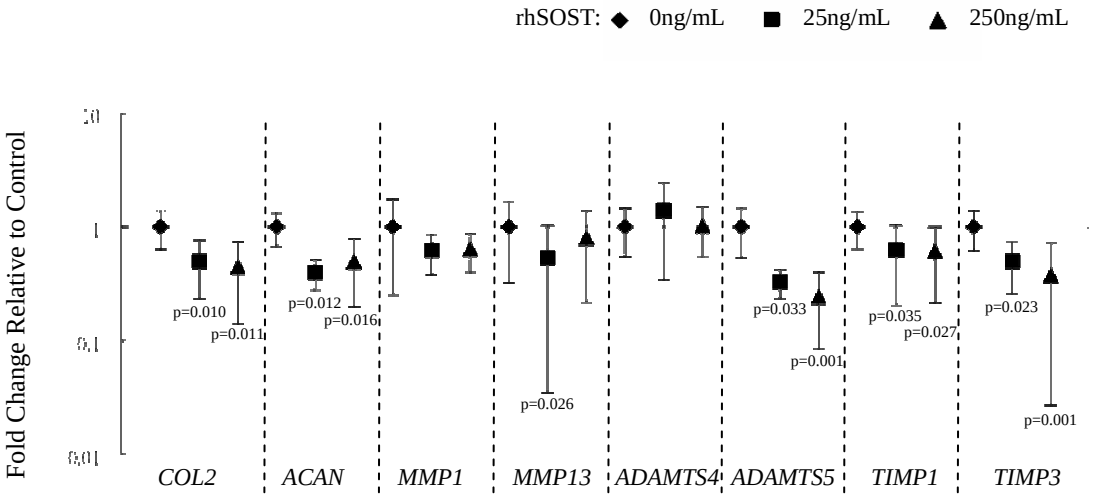
rhSOST: 0ng/mL 25ng/mL 250ng/mL
Fold Change Relative to Control
p=0.010
p=0.011
p=0.012
p=0.016
p=0.026
p=0.033
p=0.001
p=0.035
p=0.027
p=0.023
p=0.001
COL2
ACAN
MMP1
MMP13
ADAMTS4
ADAMTS5
TIMP1
TIMP3

Figure 6

A

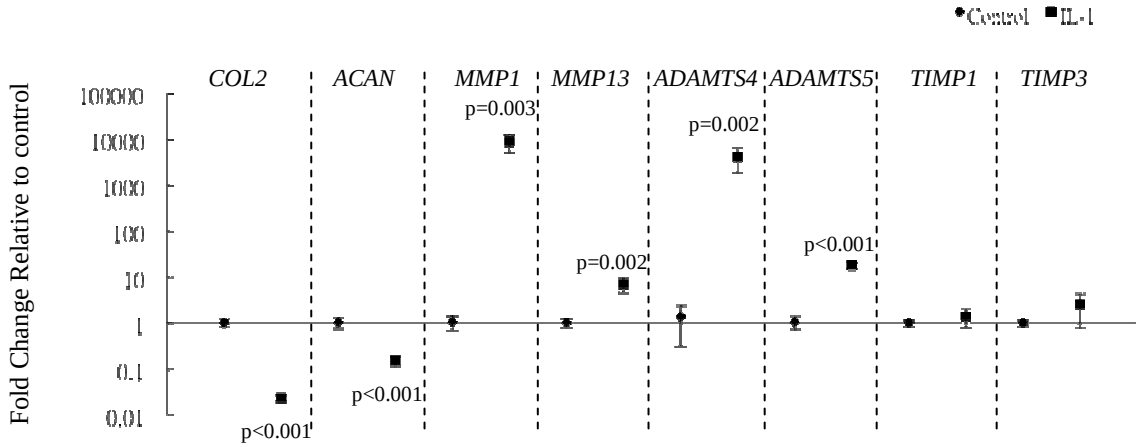
Control
IL-1
COL2
ACAN
MMP1
MMP13
ADAMTS4
ADAMTS5
TIMP1
TIMP3
Fold Change Relative to control
100000
10000
1000
100
10
1
0.1
0.01
p=0.003
p=0.002
p=0.002
p<0.001
p<0.001
p<0.001

B

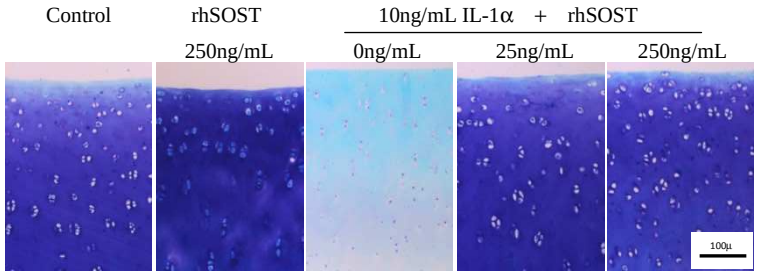
Control
rhSOST
250ng/mL
10ng/mL IL-1α + rhSOST
0ng/mL
25ng/mL
250ng/mL
100μ

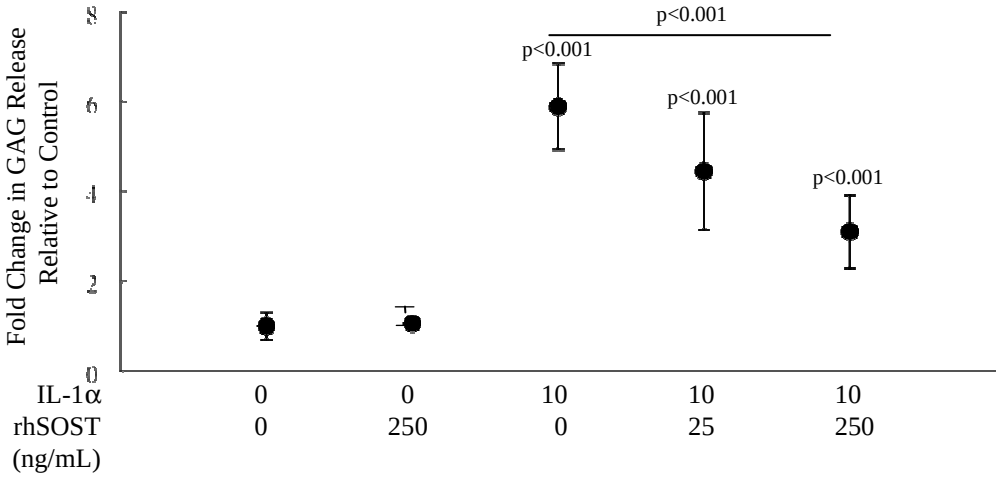
Fold Change in GAG Release Relative to Control
8
6
4
2
0
p<0.001
p<0.001
p<0.001
p<0.001
IL-1α 0 0 10 10 10
rhSOST 0 250 0 25 250
(ng/mL)

C

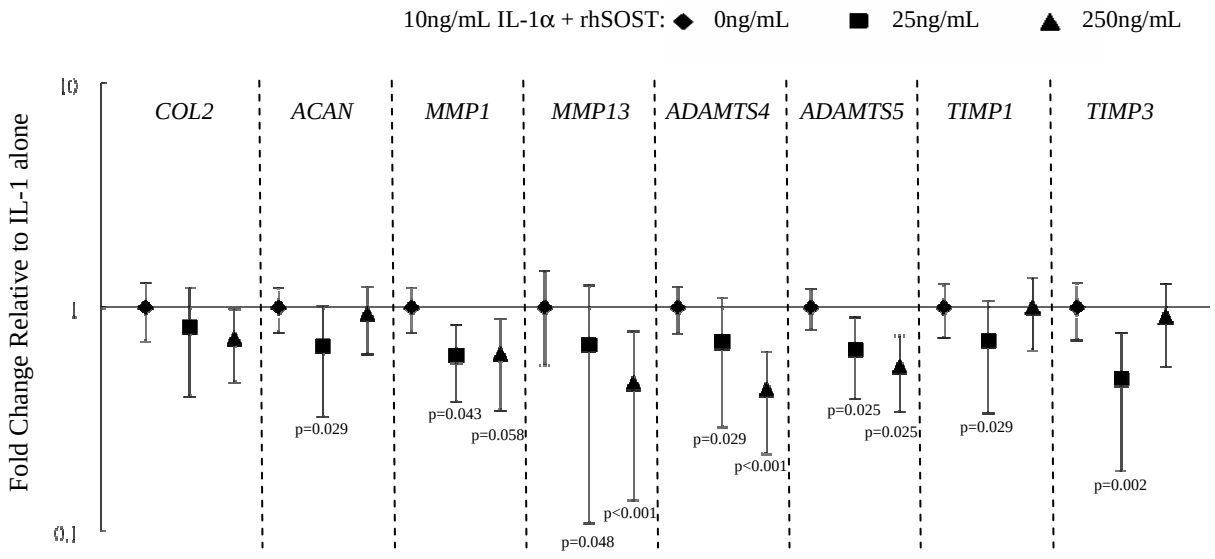
10ng/mL IL-1α + rhSOST: 0ng/mL 25ng/mL 250ng/mL
Fold Change Relative to IL-1 alone
10
1
0.1
COL2
ACAN
MMP1
MMP13
ADAMTS4
ADAMTS5
TIMP1
TIMP3
p=0.029
p=0.043
p=0.058
p=0.048
p<0.001
p=0.029
p<0.001
p=0.025
p=0.025
p=0.029
p=0.002